


## ORIGINAL ARTICLE

# Cytisine is neuroprotective in female but not male 6-hydroxydopamine lesioned parkinsonian mice and acts in combination with 17- $\beta$ -estradiol to inhibit apoptotic endoplasmic reticulum stress in dopaminergic neurons

Sara M. Zarate<sup>1</sup> | Gauri Pandey<sup>1</sup> | Sunanda Chilukuri<sup>1</sup> | Jose A. Garcia<sup>1</sup> |  
Brittany Cude<sup>1</sup> | Shannon Storey<sup>1</sup> | Nihal A. Salem<sup>1,2</sup> | Eric A. Bancroft<sup>1</sup> |  
Michelle Hook<sup>1,2</sup> | Rahul Srinivasan<sup>1,2</sup> 

<sup>1</sup>Department of Neuroscience & Experimental Therapeutics, College of Medicine, Texas A&M University, Bryan, TX, USA

<sup>2</sup>Texas A&M Institute for Neuroscience (TAMIN), College Station, TX, USA

## Correspondence

Rahul Srinivasan, Department of Neuroscience & Experimental Therapeutics, Bryan, TX 77801, USA.  
Email: rahul@tamu.edu

## Funding information

American Parkinson Disease Association; National Institute of Neurological Disorders and Stroke, Grant/Award Number: R01NS115809-01

## Abstract

Apoptotic endoplasmic reticulum (ER) stress is a major mechanism for dopaminergic (DA) loss in Parkinson's disease (PD). We assessed if low doses of the partial  $\alpha 4\beta 2$  nicotinic acetylcholine receptor agonist, cytosine attenuates apoptotic ER stress and exerts neuroprotection in substantia nigra pars compacta (SNc) DA neurons. Alternate day intraperitoneal injections of 0.2 mg/kg cytosine were administered to female and male mice with 6-hydroxydopamine (6-OHDA) lesions in the dorsolateral striatum, which caused unilateral degeneration of SNc DA neurons. Cytosine attenuated 6-OHDA-induced PD-related behaviors in female, but not in male mice. We also found significant reductions in tyrosine hydroxylase (TH) loss within the lesioned SNc of female, but not male mice. In contrast to female mice, DA neurons within the lesioned SNc of male mice showed a cytosine-induced pathological increase in the nuclear translocation of the pro-apoptotic ER stress protein, C/EBP homologous protein (CHOP). To assess the role of estrogen in cytosine neuroprotection in female mice, we exposed primary mouse DA cultures to either 10 nM 17- $\beta$ -estradiol and 200 nM cytosine or 10 nM 17- $\beta$ -estradiol alone. 17- $\beta$ -estradiol reduced expression of CHOP, whereas cytosine exposure reduced 6-OHDA-mediated nuclear translocation of two other ER stress proteins, activating transcription factor 6 and x-box-binding protein 1, but not CHOP. Taken together, these data show that cytosine and 17- $\beta$ -estradiol work in combination to inhibit all three arms (activating transcription factor 6, x-box-binding protein 1, and CHOP) of apoptotic ER stress signaling in DA neurons, which can explain the neuroprotective effect of low-dose cytosine in female mice.

**Abbreviations:** 6-OHDA, 6-hydroxydopamine; A.U., arbitrary units; ATF6, activating transcription factor 6; CHOP, C/EBP homologous protein; d.i.v., days in vitro; D1R, dopamine receptor 1; DA, dopaminergic; DLS, dorsolateral striatum; ED14, embryonic day 14; eIF2 $\alpha$ , eukaryotic initiation factor 2 $\alpha$ ; ER, endoplasmic reticulum; ERES, endoplasmic reticulum exit sites; HV, high voltage; i.p., intraperitoneal; IRE1 $\alpha$ , inositol requiring enzyme 1 $\alpha$ ; MSN, medium spiny neuron; nAChR, nicotinic acetylcholine receptor; NMDA, N-methyl-D-aspartate; PBS, phosphate-buffered saline; PD, Parkinson's disease; PERK, protein kinase RNA-linked ER kinase; ROI, region of interest; S100B, S100 calcium-binding protein B; Sec24D-ERES, Sec24D-containing endoplasmic reticulum exit sites; SNc, substantia nigra pars compacta; TH, tyrosine hydroxylase; VTA, ventral tegmental area; WT, wild-type; XBP1, x-box-binding protein.

Sara M. Zarate and Gauri Pandey contributed equally.



## KEYWORDS

6-OHDA, cytosine, dopamine, endoplasmic reticulum stress, Parkinson's disease, sex differences

## 1 | INTRODUCTION

Parkinson's disease (PD) is caused by the loss of substantia nigra pars compacta (SNc) dopaminergic (DA) neurons (Surmeier, 2018). DA neurons normally possess high levels of cellular and oxidative stress because of multiple factors such as hyperoxidative metabolites of dopamine, intracellular iron, cyclical  $\text{Ca}^{2+}$  fluxes, and protein overload (Dias et al., 2013). Further toxic insults can give rise to an unchecked endoplasmic reticulum (ER) stress response, resulting in rapid neuronal loss (Colla, 2019; Mercado et al., 2013, 2016; Wang & Takahashi, 2007). In support of this view, a pathological increase in the phosphorylation of two ER stress response proteins, protein kinase RNA-linked ER kinase (PERK) and eukaryotic initiation factor 2 $\alpha$ , which are known to activate the apoptotic ER stress protein CHOP has been reported in SNc DA neurons from postmortem brains of humans with PD (Hoozemans et al., 2007, 2012). In addition, pathological increases in ER stress signaling have also been observed in human, mouse, and rat models of PD (Colla, Coune, et al., 2012; Colla, Jensen, et al., 2012; Coppola-Segovia et al., 2017; Fernandes et al., 2016; Gully et al., 2016; Heman-Ackah et al., 2017), as well as in fruit flies with parkin mutations (Celardo et al., 2016). Together, these studies converge on the idea that apoptotic ER stress is a major mechanism for DA neuron loss and that attenuating apoptotic ER stress can be a translationally viable neuroprotective strategy for PD.

The ER stress response signaling pathway consists of three parallel signaling arms that are regulated by three ER-resident stress sensors; activating transcription factor 6 (ATF6), inositol requiring enzyme 1 $\alpha$ , and protein kinase RNA-like ER kinase (PERK). Activation of each of these three ER stress response signaling pathways culminates in the nuclear transcription of proteins that modulate protein burden in the ER (Hetz & Papa, 2018; Walter & Ron, 2011). Although protective at moderate levels of activity (Hetz & Saxena, 2017), uncontrolled activation of the three ER stress sensors and their respective downstream signaling pathways is apoptotic (Allagnat et al., 2010; Galindo et al., 2012; Gully et al., 2016; Nakanishi et al., 2005; Silva et al., 2005; Xiong et al., 2017; Zeng et al., 2009). Upon activation, ATF6 undergoes N-terminal cleavage and translocates to the nucleus, whereas the activation of inositol requiring enzyme 1 $\alpha$  and PERK result in the nuclear translocation of downstream transcription factors, x-box-binding protein (XBP1), and C/EBP homologous protein (CHOP), respectively. Since ATF6, XBP1, and CHOP can cause cell death via independent apoptotic pathways, one approach for neuroprotection is to identify drugs that can attenuate the uncontrolled translocation of ATF6, XBP1, and CHOP into nuclei of DA neurons.

We previously showed that exposure of mouse DA neurons to smoking-relevant concentrations of nicotine, incapable of activating neuronal nicotinic acetylcholine receptors (nAChRs) attenuated

tunicamycin-induced ER stress by inhibiting the nuclear translocation of ATF6, XBP1, and CHOP (Srinivasan, Henley, et al., 2016). Based on these findings, we surmised that nicotine inhibits apoptotic ER stress by chaperoning nAChRs out of the ER. Nicotine-induced nAChR chaperoning up-regulates Sec24D containing ER exit sites (Sec24D-ERES), which can alter protein flux from the ER of DA neurons, thereby attenuating pathological ER stress (Henderson et al., 2014; Srinivasan, Henley, et al., 2016; Srinivasan et al., 2011, 2012). Although our studies predict that nicotine is a viable drug for neuroprotection, clinical trials with nicotine patches have failed because of adverse effects in PD patients (Clemens et al., 1995; Lemay et al., 2003; Ma et al., 2017; Vieregge et al., 2001; Villafane et al., 2007, 2018).

The nicotinic ligand, cytosine is a potential alternative for neuroprotection in PD. Cytosine is a smoking cessation drug with a safe clinical profile (Tutka et al., 2019; Tutka & Zatonski, 2006), picomolar-binding affinity for nAChRs (Coe et al., 2005), and the ability to efficiently up-regulate  $\alpha 4\beta 2$  nAChRs (Henderson et al., 2014; Richards et al., 2011, 2012; Srinivasan et al., 2011, 2012). Based on these favorable properties, we asked if low-dose cytosine treatment is neuroprotective in a mouse model of 6-hydroxydopamine (6-OHDA)-induced parkinsonism. We found that low doses of intraperitoneally (i.p.) injected cytosine attenuated 6-OHDA-related motor deficits and SNc DA neuron loss, but only in female mice. We also found that the major estrogen metabolite, 17- $\beta$ -estradiol reduced CHOP expression in DA neurons, whereas cytosine attenuated the 6-OHDA-induced nuclear translocation of ATF6 and XBP1. Taken together, our results suggest that the combined inhibitory effect of cytosine and 17- $\beta$ -estradiol on all three arms of apoptotic ER stress signaling in SNc DA neurons can exert neuroprotection in female parkinsonian mice. Thus, combining nAChR chaperones with estrogen analogs can be developed as a new class of neuroprotective drugs for PD.

## 2 | MATERIALS AND METHODS

### 2.1 | Mice

All experiments were conducted in accordance with Texas A&M University IACUC regulations and protocols (protocol # 2019-0346) and were not pre-registered. Non-gonadectomized wild-type C57BL/6 female mice, and wild-type C57BL/6 male mice were used in behavioral studies. All mice were obtained from Taconic (Taconic), and were 8 weeks old at the start of behavioral studies. Food and water were provided ad libitum. Mice were housed with littermates in ventilated cages and maintained on a 12 hr light-dark cycle. Timed pregnant mice for generating dopaminergic (DA) cultures



were obtained from the Texas A&M Institute for Genomic Medicine (TIGM). All survival surgeries were conducted with continuous isoflurane anesthesia. Routine surgical procedures included application of eye lubricant, and administration of i.p. saline following surgeries. Pain and suffering was minimized in 6-OHDA-treated animals by providing moistened peanut butter mush kept on the cage floor to prevent weight loss following lesions. We did not administer analgesics or antibiotics to the mice in order to avoid the possibility of drug-drug interactions, which may alter the pharmacokinetics of cytosine. For generating DA cultures, timed pregnant mice were asphyxiated with carbon dioxide within 2–3 min and a secondary euthanasia with cervical dislocation was performed prior to extracting embryos. No randomization was performed to allocate subjects in the study.

## 2.2 | Procedure for striatal injections of 6-OHDA in mice

6-OHDA was stereotactically injected into the mouse dorsolateral striatum (DLS) using previously described methods (Srinivasan et al., 2015; Srinivasan, Lu, et al., 2016). A 5 mg/ml stock solution of 6-OHDA (Sigma, St. Louis, MO) was prepared in 0.9% saline with 0.2% ascorbic acid and frozen at  $-80^{\circ}\text{C}$  until use. Two microliters of the stock solution were withdrawn into a beveled glass injection pipette using a motorized Pump 11 Pico Plus Elite pump (Harvard Apparatus), attached to a stereotaxic frame (Kopf Instruments). Mice were anesthetized using isoflurane dispensed through a SomnoSuite Low Flow Anesthesia System (Kent Scientific). 6-OHDA was unilaterally injected into the DLS at a rate of 750 nl/min. Coordinates for

6-OHDA injections into the DLS were 0.8 mm anterior to bregma, 2.0 mm lateral to midline, and 2.4 mm ventral to the pial surface.

## 2.3 | Protocol for *in vivo* mouse experiments

Figure 1a shows the protocol for *in vivo* experiments in mice. Starting one week prior to 6-OHDA treatment (day  $-7$ ), female and male mice were injected intraperitoneally (i.p.), on alternate days, with 200  $\mu\text{l}$  of either 0.9% normal saline or 0.2 mg/kg  $(-)$  cytosine (Sigma), dissolved in 0.9% normal saline. Mice were weighed on alternate days, just prior to i.p. cytosine or saline injections and over the course of the entire experiment. Behavioral assays were performed on days  $-7$  (baseline), 7, 14, and 21 where day 0 is the time point for 6-OHDA injection. After testing on day 21 all mice were deeply anesthetized with isoflurane and perfused with 10% formalin. Following perfusion, midbrain sections were collected for quantification of SNc DA neurons after tyrosine hydroxylase (TH) immunostaining.

## 2.4 | Apomorphine rotations

Each mouse was placed in a 5-gallon circular bucket (33 cm diameter), and allowed to acclimate for at least 15 min prior to testing. For testing, apomorphine (0.5 mg/kg in 0.9% saline; Sigma, cat # 1041008) was injected i.p. and immediately afterward, contralateral rotational behavior was video recorded for 15 min with a ceiling mounted camcorder (Movies S1, S2). The total number of contralateral rotations made during this 15-min test was counted using Ethovision XT

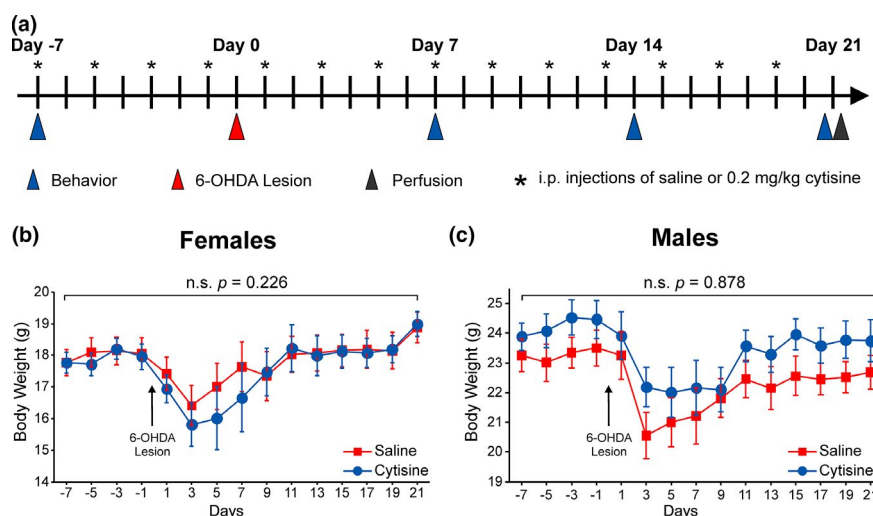


**FIGURE 1** Cytosine does not alter weight in female and male mice. (a) Schematic showing the experimental protocol for *in vivo* experiments. Female and male mice were injected intraperitoneally (i.p.) with 0.2 mg/kg cytosine on alternate days, starting on day  $-7$  (indicated by \*). Behavior was done on days  $-7$ , 7, 14, and 21 (blue arrowhead) and striatal 6-hydroxydopamine (6-OHDA) lesion was performed on day 0 (red arrowhead). Mice were perfused and brains were extracted for tyrosine hydroxylase (TH) staining on day 21 (black arrowhead) (b and c) Line graphs showing the body weight for saline and cytosine-treated female or male mice during the 28-day experiment. Error bars are S.E.M. For (b) and (c),  $p$  values are based on a two-way repeated measures ANOVA examining the interaction between treatment and time.  $n = 9$  saline and 11 cytosine females; 11 saline and 8 cytosine males

(Noldus, RRID:SCR\_000441). All detection settings on Ethovision were maintained across cohorts of mice and experiment days.

## 2.5 | Ladder rung walking test and analyses

A custom-made apparatus with 0.5-cm-thick plexiglass sidewalls encasing 33 metal dowel rungs (0.5 cm diameter, evenly spaced at 1.5 cm intervals), was used for the ladder rung walking test (Figure 2f and Movies S3, S4). Mice were video recorded while walking across the ladder rungs, freely in both directions, for 2.5 min. Video recordings were analyzed *post hoc* for gait patterns and footslips.

For gait pattern analysis, an alphabetical value was assigned to each paw: right forepaw = a, right hindpaw = b, left forepaw = c, left

hindpaw = d. A normal gait pattern was identified as movement of a forepaw (a or c) followed by movement of the contralateral hindpaw (b or d) or movement of a hindpaw (b or d) followed by the contralateral forepaw (a or c). Thus, examples of normal gait patterns are a-d-c-b or c-b-a-d (Movie S3), whereas abnormal gait patterns are a-c-b-d or c-a-d-b (Movie S4) (Figure 2d). Alphabetical scoring of gait patterns was used to determine the percent times that mice displayed normal versus abnormal gait on days -7, 7, 14 and 21.

For foot slip analysis, the number of forepaw foot slips were manually scored when the mouse was walking in a straight direction (Figure 2f). Foot slips that occurred during behaviors such as turning, rearing, or when the mouse was stationary were not counted. The foot slip data shown in Figure 2g are the fold change from baseline foot slips observed on day -7.

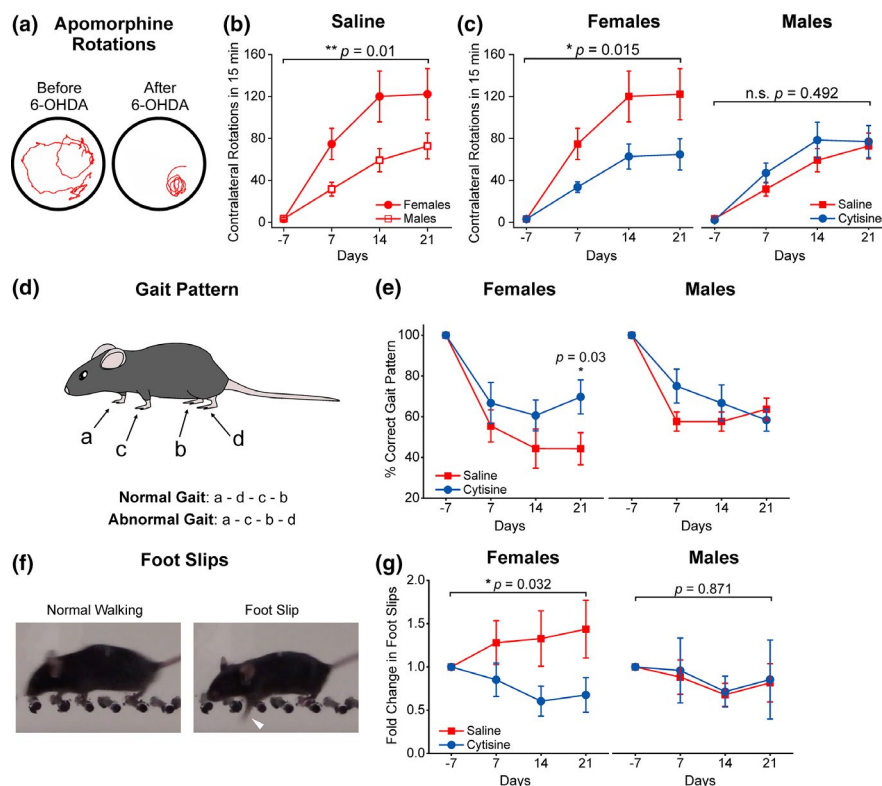


**FIGURE 2** Cytisine attenuates Parkinson's disease (PD)-related motor behaviors only in female mice. (a) Representative traces of contralateral rotations in a female mouse injected with 0.5 mg/kg apomorphine, i.p. prior to 6-hydroxydopamine (6-OHDA) lesion (left) and 21 days after unilateral 6-OHDA lesioning of the striatum (right). In contrast to the wide rotations observed prior to 6-OHDA treatment, mice show tight rotations after 6-OHDA lesioning. (b) Line graph showing apomorphine-induced rotations in saline-treated female and male mice prior to 6-OHDA lesion (day -7) and following unilateral lesioning with 6-OHDA in the striatum (days 7, 14, and 21). (c) Line graphs comparing apomorphine-induced rotations in saline versus cytosine-treated female and male. Cytisine significantly reduces apomorphine rotations only in 6-OHDA-treated females with no effect on male mice. (d) Schematic showing the method for quantifying gait patterns in mice using a horizontal ladder walking assay. (e) Line graphs showing % correct gait patterns in saline- and cytosine-treated female and male mice. 6-OHDA significantly decreases the % of correct gait in saline-treated females and males. Cytisine-treatment significantly attenuates incorrect gait pattern when compared with saline-treated females 21 days after 6-OHDA exposure, whereas there is no attenuation in cytosine-treated male mice. (f) Photographs of a female mouse walking normally on a horizontal ladder (left) and with a foot slip on the ladder (white arrowhead, right). (g) Line graphs showing a significant decrease in foot slips for female mice treated with cytosine, whereas male cytosine-treated mice show no difference in foot slips compared to saline-treated males. Error bars are S.E.M. In (b), *p* values are based on a two-way repeated measures ANOVA test with a main effect of sex and time. In (c), *p* values are based on a two-way repeated measures ANOVA with a main effect of treatment and time. In (e), *p* values are based on a Mann-Whitney test. In (g), *p* values are based on a two-way repeated measures ANOVA; *n* = 9 saline and 11 cytosine females; 11 saline and 8 cytosine males



## 2.6 | Long-term primary DA-astrocyte co-cultures

Each independent primary mouse DA astrocyte co-culture consisted of pooled midbrain cells derived from mouse embryos of four to seven timed pregnant mice at embryonic day 14. Dissociated midbrain cells from each pooled culture were plated on 8 to 10 #1 12 mm diameter glass coverslips. To obtain DA-astrocyte co-cultures, the ventral midbrain was dissected from mouse embryos as previously reported (Bancroft & Srinivasan, 2020; Henley et al., 2017; Srinivasan, Henley, et al., 2016). Following dissection, cells were dissociated using papain (Worthington Biochemical Corporation, cat # L5003126), DNase treatment (Sigma, cat # DN25), and mechanical trituration. 200,000 cells were plated on the coverslips coated with poly-L-lysine (Sigma, cat # P4832), poly-L-ornithine (Sigma, cat # P4957), and laminin (Sigma, cat # L2020). Cells were maintained in culture with neurobasal medium (ThermoFisher, cat # 21103049) supplemented with B-27 supplement (ThermoFisher, cat # 17504044), 5% heat-inactivated horse serum (ThermoFisher, cat # 26050088), GlutaMAX (ThermoFisher, cat # 35050061), 0.2% L-ascorbic acid (Sigma, cat # A7506), 10,000 U/mL penicillin-streptomycin (ThermoFisher, cat # 15140122), 60 mg/ml kanamycin (Sigma, cat # 60615), and 125 mg/ml ampicillin (Sigma, cat # A9393). Primary DA neuron astrocyte co-cultures were maintained for a total of 4 weeks and the culture medium was exchanged every 2–3 days. For ER stress marker experiments, cultures were treated with 200 nM cytosine (Sigma, cat # 5052270001) dissolved in phosphate-buffered saline (PBS) for 2 weeks starting on day in vitro 14 (d.i.v 14). On d.i.v 26, experimental cultures were treated with 400  $\mu$ M 6-OHDA dissolved in PBS containing 0.2% ascorbic acid (Sigma, cat # H4381), 400  $\mu$ M 6-OHDA for 48 hr + 200 nM cytosine for 2 weeks or 10  $\mu$ M doxorubicin for 48 hr (Sigma, cat # D1515). For 17- $\beta$ -estradiol experiments, cultures were treated with 10 nM 17- $\beta$ -estradiol, dissolved in 100% ethanol (Sigma, cat # E2758) + 200 nM cytosine for 2 weeks and on d.i.v 26, some cultures were treated with 400  $\mu$ M 6-OHDA for 48 hr. On average, our 4-week-old long-term primary DA-astrocyte co-cultures yielded 20%–30% TH positive neurons.

## 2.7 | Immunostaining

Antibodies for Sec24D and ER stress markers (ATF6, XBP1, CHOP) have been previously validated (Srinivasan, Henley, et al., 2016). For staining DA cultures, cells were fixed in 10% formalin (VWR, cat # CA71007-348) for 20 min at RT, rinsed in PBS and permeabilized with 0.01% Triton X-100 for 1 min at RT. Cultures were blocked with 10% normal goat serum (NGS) (Abcam, cat # ab7481, RRID:AB\_2716553) for 40 min at RT and incubated with the appropriate primary antibody in 1% NGS at 4°C, overnight. Primary antibodies were chicken anti-TH (1:1,500; Abcam, cat # ab76442, RRID:AB\_1524535), rabbit anti-CHOP (1:500; Abcam, cat # ab10444, RRID:AB\_2245733), rabbit anti-ATF6 (1:500; Abcam, cat # ab203119, RRID:AB\_2650448), rabbit anti-XBP1 (1:500; Abcam, cat # ab37152, RRID:AB\_778939), rabbit anti-Sec24D (1:500; ThermoFisher, cat # PA5-65793,

RRID:AB\_2662256), and rabbit anti-cleaved caspase-3 (1:500; Cell Signaling, cat # 9661S, RRID:2341188). Cells were then incubated with the appropriate secondary antibody in 1% NGS for 1 hr at RT with constant agitation. The secondary antibodies were goat anti-chicken Alexa Fluor 594 (1:2000; Abcam, cat # ab150176, RRID:AB\_2716250) and goat anti-rabbit Alexa Fluor 488 (1:1,000; Abcam, cat # ab150077, RRID:AB\_2630356). Staining for each protein was performed sequentially to prevent cross reactivity. To detect ER stress markers ATF6, XBP1, and CHOP, cultures were first labeled with primary and secondary antibodies for the stress markers, followed by TH primary and secondary antibodies. For Sec24D-ERES staining, cultures were first labeled with TH primary and secondary antibodies followed by Sec24D primary and secondary antibodies.

For immunostaining brain sections, mice were deeply anesthetized with isoflurane and transcardially perfused with 1X PBS followed by 10% formalin. Brains were extracted and stored overnight at 4°C in 10% formalin, then dehydrated for 48 hr in 30% sucrose (Sigma, cat # S7903). Midbrain sections (40  $\mu$ m) were obtained (Microm HM 550 cryostat, ThermoFisher) and stored in 0.01% sodium azide (Sigma, cat # S2002) at 4°C until immunostaining. Following 3 $\times$  washes with PBS, sections were permeabilized and blocked with 0.5% Triton X-100 + 10% normal goat serum for 1 hr at RT. Sections were co-labeled with rabbit anti-CHOP (1:500; Abcam, cat # ab10444, RRID:AB\_2245733) and a chicken anti-TH primary antibody (1:1,500, cat # ab76442) overnight at 4°C followed by a goat anti-rabbit Alexa Fluor 488 (1:1,000, Abcam, cat # ab150077, RRID:AB\_2630356) and goat anti-chicken Alexa Fluor 594 secondary antibody (1:2000, cat # ab150176, RRID:AB\_2716250) for 1 hr at RT.

## 2.8 | Confocal imaging

Imaging was performed on an inverted Olympus FV1200 confocal laser scanning microscope (Olympus) equipped with a 10 $\times$  air objective (NA 0.40), a 60 $\times$  oil immersion objective (NA 1.35) and 488 and 594 nm laser lines. Microscope settings were optimized to obtain non-saturated images, and the same settings for laser power, high voltage, gain, offset, and aperture diameter were maintained across all imaging sessions. For imaging ER stress markers (ATF6, XBP1, and CHOP), images of individual TH<sup>+</sup> cell bodies were acquired at 60 $\times$  magnification and a digital zoom of 5–8 $\times$ . DA neurons were individually imaged utilizing TH fluorescence as a guide to focus on an optical plane with the nucleus sharply demarcated. Thirty to 40 individual TH<sup>+</sup> neurons from each coverslip were imaged. For Sec24D ERES imaging, z-stacks of individual TH<sup>+</sup> neurons were obtained with a 0.45  $\mu$ m step size, and 30–40 TH<sup>+</sup> cells for each condition were imaged. Average data for each condition (Figures 4–7) were obtained from 60 to 200 TH<sup>+</sup> neurons, derived from three to four independent long-term DA cultures.

To quantify neuroprotection of the SNc after in vivo behavioral testing, TH<sup>+</sup> SNc and ventral tegmental area montages were





acquired from six midbrain sections per mouse. Montages were stitched from individual images obtained at 10x magnification, spanning the lesioned and unlesioned hemispheres (Figure 3a). Images for each montage were acquired at a single optical plane. The laser power, high voltage, gain, offset, and aperture diameter were adjusted so that pixels were not saturated and imaging parameters were maintained across all sections and mice.

## 2.9 | Image analysis

All image analysis was performed using ImageJ software. To analyze Sec24D-ERES, a z projection was generated for each TH<sup>+</sup> neuron and Sec24D-labeled ERES structures were manually thresholded. Sec24D-ERES regions of interest (ROIs) were demarcated using the Analyze Particles feature in ImageJ with a ROI area constraint of

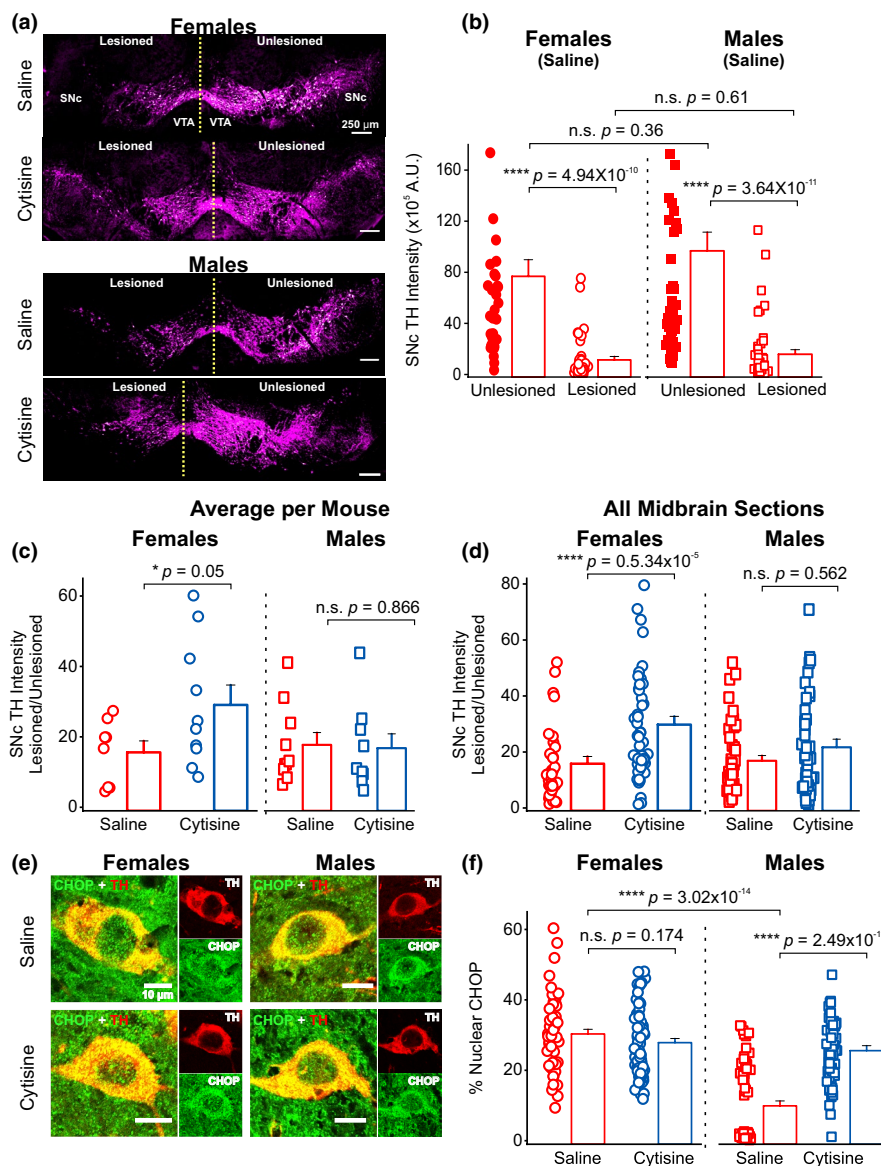


**FIGURE 3** Cytisine reduces substantia nigra pars compacta (SNc) dopaminergic (DA) neuron loss only in female mice. (a) Representative stitched confocal montages of tyrosine hydroxylase (TH)-stained midbrain sections from saline and cytosine-treated female and male mice. Regions of interest (ROIs) were manually demarcated around either the lesioned or unlesioned substantia nigra pars compacta (SNc). Note that for quantification, we also considered TH-stained DA neuron processes that extend into the substantia nigra pars reticulata (SNr). Scale bar is 250  $\mu$ m. (b) Bar graphs showing SNc TH intensity in the 6-hydroxydopamine lesioned and unlesioned side of saline-treated female and male mice. (c) and (d) Bar graphs comparing ratios of SNc TH intensities; data points represent the average of six midbrain sections per mouse in (c) or a single midbrain section and six midbrain sections were analyzed per mouse in (d). (e) Representative confocal images of TH neurons co-stained with C/EBP homologous protein (CHOP). Merged images for saline or cytosine-treated female and male mice are shown alongside individual images for TH and CHOP. Scale bar is 10  $\mu$ m. (f) Bar graphs showing % nuclear CHOP; each data point is the ratio of nuclear CHOP intensity versus whole-cell CHOP intensity. All  $p$  values are based on Mann-Whitney test and error bars are S.E.M.; for (b), (c), (d)  $n = 9$  saline and 11 cytosine females; 11 saline and 8 cytosine males; for (f)  $n = 60$  cells from saline-treated females and 69 cells from cytosine-treated females mice;  $n = 65$  saline-treated males and 70 cells from cytosine-treated males

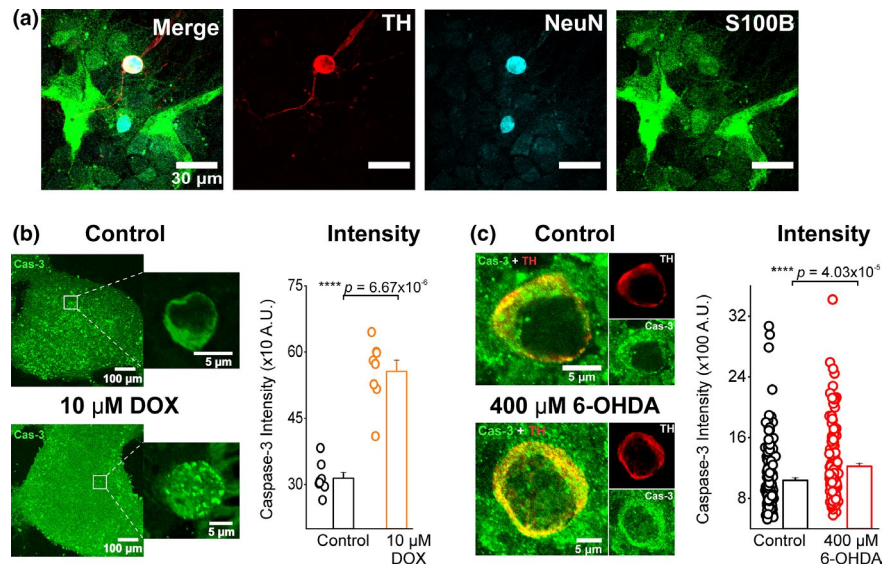


**FIGURE 4** 6-Hydroxydopamine (6-OHDA) initiates apoptosis in primary cultures of mouse dopaminergic (DA) neurons. (a) Representative confocal image of primary mouse DA neuron cultures showing a single tyrosine hydroxylase (TH)<sup>+</sup> DA neuron that is also NeuN<sup>+</sup> and a TH<sup>-</sup>, non-DA neuron that is NeuN<sup>+</sup>. The primary DA cultures also contain a monolayer of S100B<sup>+</sup> astrocytes. Scale bar is 30 µm. (b) Representative confocal images of control and 10 µM doxorubicin-treated primary mouse DA cultures stained for cleaved caspase-3 (green). Scale bar, 100 µm. Insets show individual neurons from primary mouse DA cultures stained for cleaved caspase-3 in control and 10 µM doxorubicin-treated cultures. Scale bar, 5 µm. Bar graphs quantifying cleaved caspase-3 intensity. The *p* value is based on a Mann-Whitney test; each data point represents a single 20x field of view; control: *n* = 7; 10 µM doxorubicin: *n* = 7. (c) Representative confocal images of control and 400 µM 6-OHDA-treated primary mouse DA cultures co-stained for TH (red) cleaved caspase-3 (green). Merged images for control and 400 µM 6-OHDA are shown alongside individual images of TH and cleaved caspase-3. Scale bar, 5 µm. Bar graph quantifying cleaved caspase-3 intensity. The *p* value is based on a Mann-Whitney test; each data point represents the whole-cell intensity; *n* = ~100 cells per condition

0.01–1,000 µm<sup>2</sup>. Sec24D-ERES ROIs were used to extract the number, area, and integrated fluorescence intensity, which is the sum of fluorescence values from all pixels within an ROI. For each experimental condition, 60–150 individual TH<sup>+</sup> cells from two to four independent mouse midbrain cultures were analyzed for ER stress markers (ATF6, XBP1 or CHOP).

The absence of TH labeling in the nucleus enabled a clear differentiation between cytosolic and nuclear compartments. ROIs were manually drawn around the nucleus and the whole-cell boundary for each TH<sup>+</sup> neuron, and the mean intensity of ATF6, XBP1, or CHOP was quantified separately for each demarcated region (Figure 5b). To assess percent nuclear translocation of CHOP in SNc DA neurons from immunostained midbrain sections of female and male mice, images of individual TH<sup>+</sup> SNc DA neurons from the 6-OHDA lesioned side of 40 µm mouse midbrain sections were acquired using a 60x oil immersion objective and 3x digital zoom. A ratio of integrated CHOP fluorescence intensity in the nucleus to the whole cell (nucleus + cytoplasm) was obtained, and percent nuclear CHOP translocation was extracted from this ratio for each DA neuron in the lesioned SNc.

To quantify TH fluorescence in midbrain sections, 10x mid-brain montages were thresholded to isolate TH<sup>+</sup> cell bodies and processes. ROIs from the thresholded images were utilized to obtain integrated fluorescence intensities for the unlesioned and the 6-OHDA lesioned side. Ratios of integrated fluorescence intensity of the 6-OHDA lesioned versus the unlesioned SNc were compared to assess the extent of neuroprotection by cytosine in female and

male mice. Ratios of fluorescence intensity were used instead of raw fluorescence intensity to reduce variability across midbrain sections and mice that can occur because of immunostaining artifacts.

## 2.10 | Sampling and statistics

All statistics except for behavioral experiments were performed using Origin 2019 (OriginLab, RRID:SCR\_014212) and R programming language (<https://www.r-project.org/>, RRID:SCR\_001905). Statistics for behavioral experiments were performed using Statistical Package for the Social Sciences (SPSS version 18; IBM, RRID:SCR\_019096). Experiments were blinded since the analysis was performed by a person other than the experimenter. As a pre-determined exclusion criterion, mice that died prior to the completion of the 28 day in vivo experimental protocol were excluded from analysis. No data points were excluded as outliers. All experiments were conducted during the day, between 9 a.m. to 6 p.m.

The mice reported in this study were tested in separate behavioral experiments across multiple cohorts. We used a total of 22 female and 23 male mice with a ~20% mortality rate after 6-OHDA lesion. Mice that died before the final day of the experiment were not used for weight measurements, behavioral assays, TH intensity, or CHOP intensity. Numbers of mice for weight measurements, behavioral assays, TH intensity, and CHOP intensity analysis were as follows: nine female saline mice, 11 female cytosine mice, 11





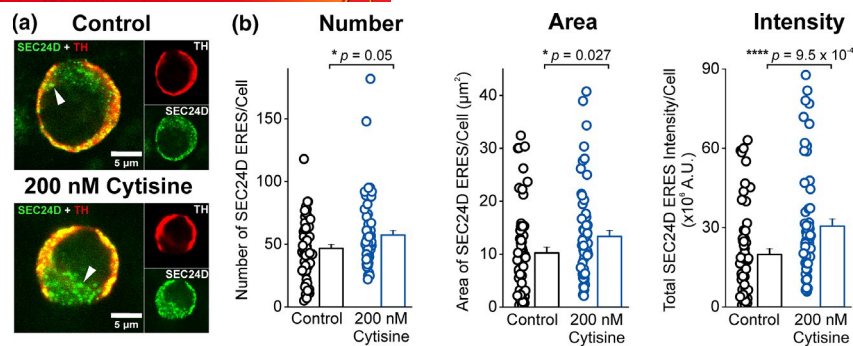


**FIGURE 6** Cytisine up-regulates Sec24D-containing ER exit sites (Sec24D-ERES) in mouse primary cultured dopaminergic (DA) neurons. (a) Representative confocal images of primary mouse DA neuron cell bodies stained for endogenous tyrosine hydroxylase (TH) (in red) and Sec24D-ERES (in green) are shown. Merged images for a control and 200 nM cytosine-treated DA neurons are shown along with separate images for TH and Sec24D staining. White arrowheads point to Sec24D-ERES puncta. Note the larger and more numerous Sec24D-ERES puncta following cytosine exposure. Scale bar is 5 μm. (b) Bar graphs quantifying the number, area, and intensity of Sec24D-ERES puncta in untreated (control) and cytosine-treated primary mouse DA cultures. All *p* values are based on Mann-Whitney test and error bars are S.E.M.; *n* = 2 independent cultures and 60 DA neurons per condition; each independent culture is from embryonic day 14 embryos derived from multiple timed pregnant mice

resampling with replacement to estimate the true distribution of a test statistic (Dwivedi et al., 2017; Maris, 2012; Wedenberg, 2013). For bootstrap analysis, the percent nuclear translocation of each of ATF6, XBP1, and CHOP in each of the experimental conditions was iteratively resampled with replacement (10,000 iterations). We tested the null hypothesis that the distribution of percent nuclear translocation for each stress marker is not different between control and experimental conditions. For each ER stress marker, *p* values were derived from the proportion of iterations in each experimental condition that exceed the mean values of the bootstrapped control condition. The null hypothesis was rejected if *p* was <.05.

### 3 | RESULTS

#### 3.1 | In vivo assessment of neuroprotection by cytosine in mice with 6-OHDA-induced parkinsonism

In order to assess if low-dose cytosine attenuates PD-related behavioral deficits, we used a mouse model of parkinsonism with unilateral loss of SNc DA neurons, induced by a unilateral injection of 6-OHDA into the dorsolateral striatum (DLS). As shown in Figure 1a, starting at 7 days prior to striatal 6-OHDA injection (day -7), mice were injected i.p. with either 0.9% saline (vehicle) or a low, 0.2 mg/kg dose of cytosine on alternate days. 6-OHDA was stereotactically injected into the DLS on day 0 and alternate day i.p. injections were continued until the mice were killed on day 21. Behavioral assays were conducted prior to cytosine and 6-OHDA treatment (day -7), and on days 7, 14, and 21 post-treatment. On day 21, the mice were perfused and 40 μm midbrain sections were obtained to quantify tyrosine hydroxylase (TH) content in the midbrain.

We first analyzed the effect of alternate day 0.2 mg/kg i.p. cytosine injections on the weight of female and male mice. No differences were observed between the weight of saline or cytosine-treated female and male mice on any day prior to or after 6-OHDA exposure.

Injection of 6-OHDA into the DLS caused a 5%–10% weight loss in saline and cytosine-treated females and males, with no observable differences in the rate of weight gain between groups of female or male mice, and no statistically significant interaction between time and treatment as the two factors tested (females:  $F_{(3,54)} = 1.496$ ;  $p = .226$ ; males:  $F_{(3,51)} = 0.226$ ,  $p = .878$ , two-way repeated measures ANOVA) (Figure 1b,c).

#### 3.2 | Cytisine attenuates apomorphine-induced rotational behavior in female mice

Intraperitoneal (i.p.) injection of apomorphine in mice with unilateral SNc lesions will increase rotations in a direction contralateral to the lesioned side. Rotation in mice occurs because of the excessive activation of hypersensitive dopamine 1 receptors in striatal medium spiny neurons (MSNs) on the lesioned side (Grealish et al., 2010). Therefore, the number of apomorphine-induced rotations can be used a quantitative measure of neuroprotection of SNc DA neurons in the 6-OHDA lesioned side. Based on this rationale, we assessed the extent of cytosine-induced neuroprotection in 6-OHDA lesioned female and male mice by quantifying the number of contralateral rotations following the systemic administration of apomorphine. All groups of mice were injected with 0.5 mg/kg apomorphine i.p., and the number of contralateral rotations were recorded for 15 min immediately after apomorphine injection (Figure 2a).

We first quantified contralateral rotations in saline-treated female and male mice. Compared to baseline rotations in mice prior to 6-OHDA lesioning, all 6-OHDA lesioned mice showed tight contralateral rotations following apomorphine injections (Figure 2a and Movies S1, S2). Rotations progressively increased from  $80 \pm 15$  on day 7 to  $118 \pm 24$  on day 21 in females and  $40 \pm 6$  on day 7 to  $80 \pm 12$  on day 21 in males (Figure 2b). Interestingly, saline-treated females showed ~twofold greater rotations when compared with saline-treated males on all days after 6-OHDA, and a significant

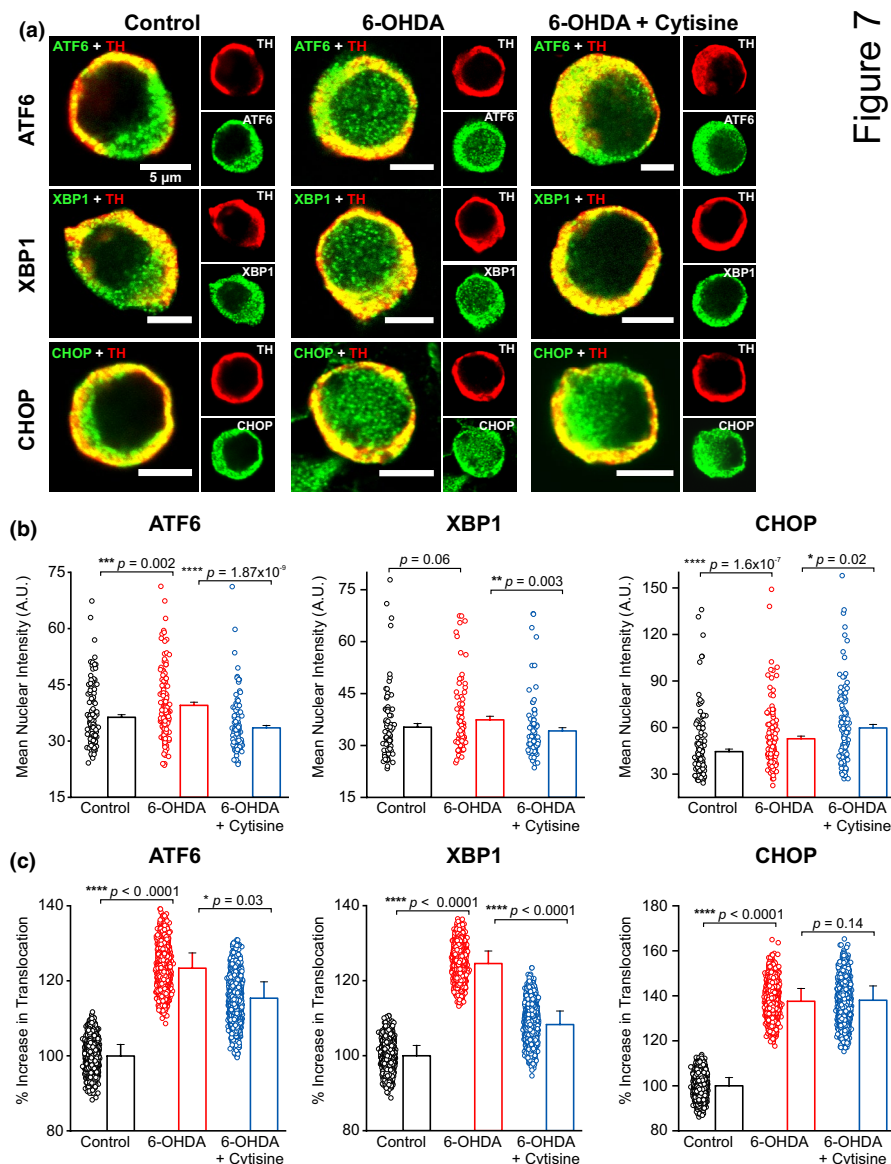


**FIGURE 7** Cytisine inhibits 6-hydroxydopamine (6-OHDA)-induced nuclear translocation of activating transcription factor 6 (ATF6) and x-box-binding protein (XBP1), but not C/EBP homologous protein (CHOP) in primary cultures of mouse dopaminergic (DA) neurons. (a) Representative confocal images of single tyrosine hydroxylase (TH)<sup>+</sup> cultured primary mouse DA neurons without any treatment (control) or with either 6-OHDA (400 μM, 48 hr) or cytosine (200 nM, 2 weeks) + 6-OHDA (400 μM, 48 hr). DA cultures were stained for TH and either ATF6 or XBP1 or CHOP and confocal images of individual TH<sup>+</sup> DA neurons were acquired as shown. Labels on columns and rows indicate treatment and staining conditions, respectively. Scale bars are 5 μm. (b) Bar graphs of population data from multiple independent cultures and DA cells showing mean nuclear intensity in single DA neurons exposed to treatment conditions and stained for ATF6, XBP1, and CHOP as shown in (a);  $n = 3$  to 4 independent cultures and ~100 DA neurons per condition;  $p$  values are based on Mann-Whitney test; each independent culture is from embryonic day 14 embryos derived from multiple timed pregnant mice. Error bars are S.E.M. (c) Bar graphs show results from bootstrap analysis for ATF6, XBP1, and CHOP with 10,000 re-sampling and replacement iterations of the experimental data from (b);  $p$  values are based on the number of times that control sample mean values differ from the test sample (see materials and methods, statistical analysis for bootstrapping); error bars are SD

interaction between time and sex ( $F_{(3,54)} = 4.141$ ;  $p = .01$ , two-way repeated measures ANOVA).

Having verified the model for apomorphine-induced rotations in mice, we assessed the effect of cytosine treatment on contralateral rotations in 6-OHDA-treated females and males. Interestingly, cytosine-treated females showed twofold fewer rotations than saline controls on days 7, 14, and 21 after 6-OHDA (Figure 2c), and significant

interaction between time and treatment ( $F_{(3,54)} = 3.834$ ;  $p = .015$ , two-way repeated measures ANOVA). In contrast, cytosine-treated males rotated to a similar extent as saline controls (Figure 2c), and no interaction between time and treatment ( $F_{(3,48)} = 0.815$ ;  $p = .492$ , two-way repeated measures ANOVA). These data demonstrate that cytosine attenuates rotational behavior only in female mice at concentrations that cannot activate nAChRs.

### 3.3 | Cytisine attenuates gait pattern only in female mice

We analyzed gait patterns for all 6-OHDA-injected mice that were subjected to rotational assays. Gait was manually determined, counting normal versus abnormal patterns, during the ladder rung walking test (Figure 2d). At baseline (day -7), all mice showed normal gait patterns 100% of the time. However, following 6-OHDA treatment, saline-treated female and male mice showed a significant 40 to 50% decline in normal gait pattern (day -7 to day 7; females:  $p = .01$ ; males:  $p = .002$ , Wilcoxon Signed Rank test) (Figure 2e and Movies S3, S4), indicating that unilateral 6-OHDA lesioning causes a significant deficit in the gait of both female and male mice.

Compared to saline controls, cytosine-treated females showed a significant 30% increase in normal gait pattern on day 21 after 6-OHDA ( $p = .03$ , Mann-Whitney test) (Figure 2e). In contrast, cytosine-treated male mice showed no improvement in gait pattern on days 7, 14, or 21 (Figure 2e). These data show that cytosine significantly attenuates gait abnormalities in 6-OHDA-treated female, but not in male mice.

### 3.4 | Cytisine reduces foot slips only in female mice

As a third behavioral measure, we quantified foot slips in all mice during the ladder rung walking test (Figure 2f). We found that cytosine-injected females displayed ~50% fewer foot slips than saline controls on days 7, 14, and 21 following 6-OHDA lesioning and a significant interaction between time and treatment ( $F_{(1,18)} = 5.39$ ;  $p = .032$ , two-way repeated measures ANOVA) (Figure 2g). In contrast, there was no effect of cytosine on foot slips in male mice (Figure 2g), and no significant interaction between time and treatment ( $F_{(1,17)} = 0.027$ ;  $p = .871$ , two-way repeated measures ANOVA).

In summary, using three independent behavioral assays, we demonstrate that chronic systemic exposure to low-dose cytosine significantly reduces PD-related motor deficits in female, but not in male parkinsonian mice.

### 3.5 | Cytisine reduces the loss of substantia nigra pars compacta (SNc) dopaminergic (DA) neurons in 6-OHDA-treated female mice

Since cytosine attenuated PD-related behaviors in female mice, we asked if cytosine exerts neuroprotection in the SNc of female mice. Midbrain sections from all mice subjected to behavioral assays were stained for tyrosine hydroxylase (TH) and montages were acquired from six midbrain sections per mouse (Figure 3a).

To assess the extent to which unilateral 6-OHDA injections induce SNc DA neuron loss in saline-treated female and male mice, we measured TH fluorescence intensity in the SNc from lesioned and unlesioned sides of midbrain sections. When compared with the unlesioned side, both female and male saline-treated mice showed an

~85% reduction in SNc TH intensity on the lesioned side (for females, integrated TH intensities in unlesioned SNc:  $7.7 \times 10^6 \pm 1.3 \times 10^6$  arbitrary units (A.U.) and in lesioned SNc:  $1.1 \times 10^6 \pm 0.27 \times 10^6$  A.U.,  $p = 4.94 \times 10^{-10}$ ; for males, integrated TH intensities in unlesioned SNc:  $9.7 \times 10^6 \pm 1.46 \times 10^6$  A.U. and in lesioned SNc:  $1.6 \times 10^6 \pm 0.36 \times 10^6$  A.U.,  $p = 3.64 \times 10^{-11}$ , Mann-Whitney test) (Figure 3a,b). No significant sex differences were observed in total SNc TH content within either the unlesioned or lesioned side of saline-treated female and male mice (unlesioned:  $p = .36$ ; lesioned:  $p = .61$ , Mann-Whitney test) (Figure 3b).

Next, we assessed if cytosine exerts a neuroprotective effect on SNc DA neurons in female mice. For each midbrain section, TH intensity ratios of the lesioned and unlesioned SNc were obtained in cytosine- and saline-treated female and male mice. The use of TH intensity ratios between lesioned and unlesioned SNc, rather than mean TH intensity in the lesioned SNc reduces variability that could occur between individual midbrain sections as a result of immunostaining procedure artifacts. When compared with saline-treated female mice, TH intensity ratios in the SNc were ~50% larger in cytosine-treated female mice, whereas cytosine- and saline-injected male mice showed no difference in TH ratios. The robust increase in SNc TH intensity ratios in cytosine-treated female mice was statistically significant regardless of whether mean TH intensity ratios were compared between individual groups of mice using an average TH intensity ratio obtained from multiple SNc midbrain sections for each mouse ( $n = 6$  SNc midbrain sections per mouse; females:  $p = .05$ ; males:  $p = .866$ , Mann-Whitney test) (Figure 3c), or when individual TH intensity ratios of the midbrain SNc were obtained for each individual section and then pooled for groups of female and male mice (females:  $p = 5.34 \times 10^{-5}$ ; males:  $p = .562$ , Mann-Whitney test) (Figure 3d). These data show that cytosine exerts a neuroprotective effect in SNc DA neurons of 6-OHDA-treated female, but not male parkinsonian mice.

### 3.6 | Cytisine treatment causes a pathological increase in the nuclear translocation CHOP only in 6-OHDA-treated male mice

Previous studies have shown that the degeneration of DA neurons by 6-OHDA requires CHOP expression (Aime et al., 2020; Silva et al., 2005). Therefore, we assessed the extent to which 6-OHDA causes the nuclear translocation of CHOP in lesioned SNc DA neurons of cytosine- and saline-treated female and male mice. DA neurons from the lesioned SNc were immunostained for CHOP and the extent of CHOP translocation into the nucleus of SNc DA neurons was assessed across all treatment groups in female and male mice (Figure 3e). We found that the percent nuclear translocation of CHOP in lesioned SNc DA neurons was significantly lower in saline-treated males when compared with saline-treated females (Figure 3f) ( $n = 60$  female and 65 male cells;  $p = 3.02 \times 10^{-14}$ , Mann-Whitney test). Furthermore, when compared with saline-treated males, cytosine-treated males showed a significant threefold increase in the percent nuclear translocation of



CHOP (Figure 3f) ( $n = 65$  saline and  $70$  cytosine cells;  $p = 2.49 \times 10^{-11}$ , Mann–Whitney test). In contrast, no significant differences were observed between saline- and cytosine-treated females for nuclear CHOP translocation in lesioned SNc DA neurons (Figure 3f) ( $n = 60$  saline and  $69$  cytosine cells;  $p = .174$ , Mann–Whitney test). Together, these data show a clear sex difference in the ability of the key pro-apoptotic ER stress molecule, CHOP to translocate into nuclei of SNc DA neurons.

### 3.7 | Exposure to 6-OHDA causes cleavage and activation of pro-apoptotic caspase-3 in cultured primary mouse DA neurons

Based on the observation that cytosine causes a robust increase in nuclear CHOP translocation in SNc DA neurons of male but not female mice, we sought to determine if estrogen regulates CHOP activation in DA neurons. To do this, we generated primary cultures of mouse DA neurons, and first assessed if exposure of primary cultured mouse DA neurons to 6-OHDA is sufficient to initiate the apoptosis of cultured TH<sup>+</sup> DA neurons. Because caspase-3 cleavage and activation is a known downstream mechanism for CHOP-mediated apoptosis (Quick & Faison, 2012; Teske et al., 2013; Wang et al., 2014), we specifically assessed the extent to which 6-OHDA induces caspase-3 cleavage in cultured midbrain DA neurons.

Primary midbrain neurons were cultured with midbrain astrocytes using previously published methods (Bancroft & Srinivasan, 2020; Henley et al., 2017; Srinivasan, Henley, et al., 2016). Our long-term 4-week-old primary mouse midbrain neuron-astrocyte co-cultures contain mature TH<sup>+</sup> and TH<sup>-</sup> neurons on a monolayer of S100B<sup>+</sup> mouse midbrain astrocytes (Figure 4a) (Bancroft & Srinivasan, 2020; Henley et al., 2017; Srinivasan, Henley, et al., 2016). Four-week-old midbrain cultures were treated with  $400 \mu\text{M}$  6-OHDA for 48 hr, and immunostained for caspase-3 using an antibody specific to the cleaved form of caspase-3 (Figure 4c). In parallel experiments, the cleaved caspase-3 antibody was validated in midbrain cultures treated with  $10 \mu\text{M}$  doxorubicin, which is known to cleave and activate caspase-3 (Ueno et al., 2006; Wei et al., 2015) (Figure 4b).  $10 \mu\text{M}$  doxorubicin caused a significant and robust increase in immunostained cleaved caspase-3 in midbrain cultures, thus validating the antibody ( $p = 6.67 \times 10^{-6}$ , Mann–Whitney test) (Figure 4b). Using this validated cleaved caspase-3 antibody, we found that 48 hr exposure to  $400 \mu\text{M}$  6-OHDA caused a significant increase in cleaved caspase-3 expression in TH<sup>+</sup> neurons ( $p = 4.03 \times 10^{-5}$ , Mann–Whitney test) (Figure 4c), indicating that 48 hr exposure to  $400 \mu\text{M}$  6-OHDA is sufficient to initiate apoptosis in primary cultured DA neurons.

### 3.8 | 17- $\beta$ -estradiol alone inhibits CHOP expression in mouse DA neurons

Having established that 6-OHDA initiates apoptosis of cultured primary mouse DA neurons, we assessed the effect of cytosine and the

major estrogen metabolite, 17- $\beta$ -estradiol on CHOP in cultured primary mouse DA neurons exposed to 6-OHDA.

Primary mouse midbrain cultures were treated with either no drug (control), 6-OHDA ( $400 \mu\text{M}$ , 48 hr), 6-OHDA ( $400 \mu\text{M}$ , 48 hr) + cytosine ( $200 \text{ nM}$ , 2 weeks), or 6-OHDA ( $400 \mu\text{M}$ ) + cytosine ( $200 \text{ nM}$ ) + 17- $\beta$ -estradiol ( $10 \text{ nM}$ , 2 weeks) and for each treatment condition, CHOP fluorescence was quantified in either the whole cell or in the nucleus of TH<sup>+</sup> DA neurons (Figure 5a,b). Population data from four independent midbrain cultures and  $\sim 100$  DA neurons per condition showed that when compared with untreated control neurons, 6-OHDA significantly increased mean CHOP fluorescence across the whole cell and in the nucleus (whole cell:  $p = 1.46 \times 10^{-5}$ ; nucleus:  $p = 8.23 \times 10^{-6}$ ; Mann–Whitney test), and pre-exposure of 6-OHDA-treated cells to cytosine failed to reduce CHOP expression in either compartment (whole cell:  $p = .84$ ; nucleus:  $p = .007$ ; Mann–Whitney test) (Figure 5b). On the other hand, co-treatment of 6-OHDA + cytosine-exposed cells with 17- $\beta$ -estradiol significantly reduced CHOP fluorescence in the whole cell and in the nucleus of DA neurons (whole cell:  $p = 7.27 \times 10^{-7}$ ; nucleus:  $p = 5.07 \times 10^{-7}$ ; Mann–Whitney test) (Figure 5b). To determine if 17- $\beta$ -estradiol alone could reduce CHOP fluorescence, DA cultures were treated with  $10 \text{ nM}$  of 17- $\beta$ -estradiol for 2 weeks, and baseline CHOP fluorescence intensities in the control and 17- $\beta$ -estradiol-treated conditions were measured. When compared with untreated control cultures, 17- $\beta$ -estradiol alone caused a significant reduction in mean CHOP fluorescence across the whole cell ( $p = .003$ ; Mann–Whitney test) (Figure 5c).

Based on these data, we conclude that 17- $\beta$ -estradiol alone decreases CHOP expression to baseline levels in cultured DA neurons, and this occurs at nanomolar concentrations that are physiologically relevant to in vivo 17- $\beta$ -estradiol concentrations.

### 3.9 | Cytosine up-regulates Sec24D-containing ER exit sites (Sec24D-ERES) in primary cultured mouse DA neurons

The observation that 17- $\beta$ -estradiol alone inhibits CHOP expression in DA neurons led us to assess the effect of cytosine on all the three key proteins, ATF6, XBP1, and CHOP that are known to play a central role in regulating each of the three arms of ER stress signaling.

Ligand-mediated chaperoning of nAChRs up-regulates Sec24D-ERES, which can reduce ER protein burden and mitigate pathological ER stress (Srinivasan, Henley, et al., 2016; Srinivasan et al., 2011, 2012). Since cytosine binds to nAChRs with picomolar affinity (Coe et al., 2005), and up-regulates  $\alpha 4\beta 2^*$  nAChRs (\* denotes other unknown pentameric nAChR subunits) (Richards et al., 2011, 2012; Srinivasan et al., 2011), we first asked if nanomolar concentrations of cytosine can chaperone nAChRs and consequently, up-regulate Sec24D-ERES in cultured DA neurons.

To assess cytosine-induced Sec24D-ERES up-regulation, DA cultures were treated with  $200 \text{ nM}$  cytosine for 2 weeks and endogenous Sec24D-ERES sites were immunolabeled and quantified with





confocal microscopy (Figure 6a). Compared to untreated control cultures, 2 weeks of cytosine exposure significantly increased the number, area, and intensity of Sec24D-ERES in TH<sup>+</sup> DA neurons ( $p = .05$  for number,  $p = .027$  for area,  $p = 9.5 \times 10^{-4}$  for intensity; Mann-Whitney test) (Figure 6b). These data demonstrate that cytosine up-regulates Sec24D-ERES in DA neurons at doses that cannot activate surface nAChRs.

### 3.10 | Cytosine attenuates the nuclear translocation of ATF6 and XBP1, but not CHOP in 6-OHDA-treated primary cultured mouse DA neurons

Four-week-old primary mouse DA neuron-astrocyte co-cultures were incubated with 400  $\mu$ M 6-OHDA for 48 hr and the nuclear translocation of three key ER stress response proteins, ATF6, XBP1, and CHOP were quantified in untreated versus 6-OHDA-treated and 6-OHDA + cytosine-treated cultures. We found that 6-OHDA significantly increased nuclear translocation of ATF6, XBP1, and CHOP in cultured primary mouse TH<sup>+</sup> neurons (ATF6:  $p = .002$ , XBP1:  $p = .06$ , CHOP:  $p = 1.6 \times 10^{-7}$ ; Mann-Whitney test) (Figure 7a,b). Co-exposure of DA cultures to cytosine (200 nM for 2 weeks) and 6-OHDA (400  $\mu$ M for 48 hr) significantly decreased nuclear ATF6 and XBP1 translocation in TH<sup>+</sup> DA neurons (ATF6:  $p = 1.87 \times 10^{-9}$ , XBP1:  $p = .003$ ; Mann-Whitney test), and caused a significant increase in nuclear CHOP fluorescence ( $p = .02$ , Mann-Whitney) (Figure 7b).

To account for variability in ER stress levels across independent primary DA cultures, we applied bootstrap analysis for all experimental data from Figure 7b. Ten thousand iterations of bootstrap re-sampling and replacement were performed using experimentally derived nuclear intensities of ATF6, XBP1, and CHOP. 6-OHDA showed a significant pathological increase in the nuclear translocation of ATF6, XBP1, and CHOP (ATF6:  $p < .0001$ , XBP1:  $p < .0001$ , CHOP:  $p < .001$ ). Consistent with the experimental data, cytosine significantly reduced the 6-OHDA-mediated increases of nuclear ATF6 and XBP1 levels with no attenuation of 6-OHDA-induced nuclear CHOP translocation (ATF6:  $p = .03$ ; XBP1:  $p < .0001$ ; CHOP:  $p = .14$ ; bootstrap analyses) (Figure 7c). Thus, chronic exposure to 200 nM cytosine attenuated only two of the three signaling arms of 6-OHDA-induced hyperactive ER stress (ATF6 and XBP1), without affecting 6-OHDA-induced CHOP activation in DA neurons.

Taken together, these results show that in cultured DA neurons, 17- $\beta$ -estradiol inhibits CHOP expression, whereas cytosine reduces the nuclear translocation of ATF6 and XBP1. Thus, the combination of 17- $\beta$ -estradiol and cytosine attenuates all three arms (ATF6, XBP1 and CHOP) of the ER stress signaling pathway in DA neurons.

## 4 | DISCUSSION

In this study, we found a novel sex difference in the ability of the nAChR ligand, cytosine to attenuate PD-related behaviors in mice at

concentrations that are incapable of activating nAChRs. We report that cytosine attenuates 6-OHDA-induced motor deficits and exerts neuroprotection only in female mice (Figures 2,3). We further show that the sex-specific neuroprotective effect of cytosine correlates with an abnormal nuclear translocation of CHOP in lesioned SNc DA neurons of male but not female mice (Figure 3f). We also find that 17- $\beta$ -estradiol is sufficient to inhibit CHOP expression (Figure 5c), whereas cytosine alone attenuates 6-OHDA-induced nuclear translocation of ATF6 and XBP1 in DA neurons (Figure 7b). In sum, our results suggest that cytosine and 17- $\beta$ -estradiol exert a combined inhibitory effect on all three arms of apoptotic ER stress signaling in DA neurons. This study lays a mechanistic foundation for developing combinations of nicotinic ligands with 17- $\beta$ -estradiol analogs as a novel neuroprotective treatment for PD.

PD demonstrates robust sex differences in the human population. Males are at a twofold higher risk for PD than females (Baldereschi et al., 2000), whereas motor abnormalities and dyskinesias have been reported as more severe in females than in males (Accolla et al., 2007; Baba et al., 2005; Hariz et al., 2003). This raises the question of whether animal models of PD recapitulate aspects of these sex differences. In this regard, we found that female mice were generally more susceptible to 6-OHDA-induced motor deficits than male mice (Figure 2b,e,g). In addition, when compared with saline-treated female mice, saline-treated male mice showed significantly fewer apomorphine-induced rotations on days 7, 14, and 21 following 6-OHDA injection (Figure 2b). Sex differences in PD-related behavioral deficits cannot be attributed to differences in the extent of SNc DA neuron loss in the lesioned side of mice, or because of sex differences in baseline SNc DA neuronal content, because both of these parameters were not significantly different between female and male mice (Figure 3b). Since apomorphine induces rotational behavior by activating hypersensitive D1 receptors on striatal MSNs in the lesioned side, high levels of estrogen in female mice likely potentiate the hypersensitization of D1 receptors on MSNs in the lesioned striatum. This is supported by studies showing estrogen can alter the response of D1 receptors to dopamine (Becker, 1990; Lammers et al., 1999; Tozzi et al., 2015). Thus, there are two distinct effects of estrogen on the dopaminergic system in vivo: (a) Neuroprotective effects of estrogen on CHOP in SNc DA neurons, and (b) Functional effects of estrogen on dopamine neurotransmission in striatal MSNs. Although we did not study the effects of progesterone on ER stress signaling in DA neurons, studies have shown that chronic treatment of mice with progesterone worsens PD symptoms in a 6-OHDA rodent model of PD (Chao et al., 2011), whereas other studies suggest a neuromodulatory rather than a neuroprotective effect of progesterone on turning behavior in rodents (Yunes et al., 2015). Estrogen and progesterone are therefore likely to interact via cell autonomous and non-cell autonomous mechanisms to mediate neuroprotection in vivo.

We used the in vivo striatal 6-OHDA model of parkinsonism in mice to show that low dose, alternate day i.p. injections of 0.2 mg/kg cytosine attenuate PD-related behavioral deficits (Figure 2c,e,g) and SNc DA neuron loss in female mice with no effect on males



(Figure 3c,d). 6-OHDA induces apoptotic ER stress in vitro and in vivo (Cai et al., 2016; Holtz & O'Malley, 2003; Hu et al., 2014; Ryu et al., 2002; Xie et al., 2012), and CHOP knockout mice treated with 6-OHDA show reduced DA neuron loss (Silva et al., 2005), which suggests that the neurodegenerative effects of 6-OHDA involve activation of apoptotic ER stress signaling and a pathological activation of CHOP.

17- $\beta$ -estradiol alone was sufficient to reduce CHOP expression levels in DA neurons (Figure 5c). The observed 17- $\beta$ -estradiol-induced reduction in whole-cell CHOP fluorescence in cultured primary DA neurons suggests that 17- $\beta$ -estradiol reduces CHOP expression either via a transcriptional mechanism or by increasing protein degradation rate. In support of this hypothesis, a recent study showed that ligand activation of estrogen receptor  $\alpha$  (ER $\alpha$ ) in pancreatic  $\beta$ -cells inhibits CHOP transcription and that the *Chop* promoter contains consensus estrogen-response element sites (Zhou et al., 2018). The ability of 17- $\beta$ -estradiol to inhibit CHOP expression in DA neurons, possibly via a transcriptional mechanism is a novel finding, and potentially important in the context of sex differences in PD. Our finding that 17- $\beta$ -estradiol inhibits CHOP expression is further supported by studies showing that estrogen receptor agonists exert neuroprotection in rodent models of 6-OHDA (Baraka et al., 2011; McFarland et al., 2013). We also found striking sex differences in the nuclear translocation of CHOP in DA neurons. Saline-treated males showed significantly lower levels of nuclear CHOP within lesioned SNc DA neurons than saline-treated females (Figure 3f). In addition, cytosine caused an abnormal increase in the nuclear CHOP translocation of male but not female mice (Figure 3f). A significant increase in nuclear CHOP was also observed in primary DA neurons treated with cytosine and 6-OHDA, but with no exposure to 17- $\beta$ -estradiol (Figure 7b). Together, these data point to a sex difference in the ability of CHOP to translocate into the nucleus of DA neurons, which is likely modulated by both cytosine and 17- $\beta$ -estradiol.

We found that cytosine exposure reduced 6-OHDA-mediated nuclear translocation of ATF6 and XBP1 (Figure 7b,c) that along with CHOP are key molecules regulating the three arms of ER stress signaling. The effects of cytosine are not likely to involve nAChR activation because the dosage regimen of cytosine used for in vivo experiments (0.2 mg/kg on alternate days) likely results in a 100–200 nM steady-state concentration of cytosine in the brain, which cannot activate, but can chaperone nAChRs. We hypothesize that the inhibitory effect of cytosine on ATF6 and XBP1 sequentially occurs because of cytosine-mediated pharmacological chaperoning of neuronal nicotinic acetylcholine receptors (nAChRs), an up-regulation of Sec24D-containing ER exit sites (Sec24D-ERES), and a generalized change in the flux of proteins from the ER. The consequent reduction in ER protein burden would allow DA neurons to endure further toxic insults, without triggering an apoptotic nuclear translocation of ATF6 and XBP1.

Several points support our hypothesis that pharmacological chaperoning of nAChRs by cytosine is the primary mechanism for attenuating the pathological translocation of ATF6 and XBP1 in DA neurons. These include: (a) Our previous study showing that 100 nM

nicotine inhibits ER stress by pharmacological chaperoning of nAChRs (Srinivasan, Henley, et al., 2016), (b) The picomolar-binding affinity of cytosine for nAChRs (Coe et al., 2005), and (c) The ability of cytosine to up-regulate endogenous Sec24D-ERES in DA neurons (Figure 6b). nAChRs account for less than 1% of the total protein content in DA neurons. Therefore, a major question is how nAChR chaperoning and Sec24D-ERES up-regulation can cause a generalized change in protein flux from the ER? A recent study shows that the up-regulated assembly of small numbers of Sec24-ERES activate a signaling cascade called autoregulation of ER export (AREX), whereby increased assembly of Sec24-ERES triggers a guanine nucleotide exchange factor-dependent signaling pathway, which coordinates the protein export machinery in cells and attenuates protein synthesis (Subramanian et al., 2019). AREX explains the ability of cytosine-bound nAChRs to globally affect protein flux in DA neurons and reduce pathological ER stress in DA neurons.

We show that 17- $\beta$ -estradiol and cytosine exert a combined inhibitory effect on the three signaling arms of the ER stress pathway. Additional mechanisms for the observed sex difference in this combined inhibitory effect include the idea that female mice might metabolize cytosine differently than males, resulting in neuroprotection, slower metabolism and excretion of cytosine in females, a novel cytosine metabolite produced only in females, or a cytosine-induced surge of brain-derived 17- $\beta$ -estradiol because of up-regulation of astrocytic aromatase in female mice. Future studies will systematically dissect these possibilities, as well as consider sex-dependent genetic factors known to exert neuroprotection in PD (Lee et al., 2019).

## ACKNOWLEDGMENTS

This study was supported by grants from the American Parkinson Disease Association (APDA) and NIH R01NS115809-01 to RS. We thank the Texas A&M Institute for Genomic Medicine (TIGM) for providing timed pregnant mice to generate primary dopaminergic cultures.

All experiments were conducted in compliance with the ARRIVE guidelines.

## CONFLICT OF INTEREST

Authors declare no competing financial interests.

## AUTHOR CONTRIBUTIONS

SMZ and GP performed behavioral experiments and analyses, dopaminergic culture work and data analyses, and contributed to writing and editing the manuscript. SMZ and GP performed CHOP and tyrosine hydroxylase staining, imaging, and analyses of mouse midbrain sections. SC, JAG, BC and SS performed behavioral experiments and analyses. NAS performed bootstrap analyses and contributed to editing the manuscript. EAB and GP cultured dopaminergic neurons. MH designed behavioral experiments, methods to analyze behavior, and contributed to editing the manuscript. RS conceived and coordinated the study, trained personnel, designed and supervised all experiments, provided resources and funding, and wrote the manuscript.



## ORCID

Rahul Srinivasan  <https://orcid.org/0000-0003-0237-6602>

## REFERENCES

- Accolla, E., Caputo, E., Cogiamanian, F., Tamma, F., Mrakic-Sposta, S., Marceglia, S., Egidio, M., Rampini, P., Locatelli, M., & Priori, A. (2007). Gender differences in patients with Parkinson's disease treated with subthalamic deep brain stimulation. *Movement Disorders*, 22, 1150–1156. <https://doi.org/10.1002/mds.21520>
- Aime, P., Karuppagounder, S. S., Rao, A., Chen, Y., Burke, R. E., Ratan, R., & Greene, L. A. (2020). The drug adaptaquin blocks ATF4/CHOP-dependent pro-death Trib3 induction and protects in cellular and mouse models of Parkinson's disease. *Neurobiology of Diseases*, 136, 104725. <https://doi.org/10.1016/j.nbd.2019.104725>
- Allagnat, F., Christulia, F., Ortis, F., Piro, P., Lortz, S., Lenzen, S., Eizirik, D. L., & Cardozo, A. K. (2010). Sustained production of spliced X-box binding protein 1 (XBP1) induces pancreatic beta cell dysfunction and apoptosis. *Diabetologia*, 53, 1120–1130. <https://doi.org/10.1007/s00125-010-1699-7>
- Baba, Y., Putzke, J. D., Whaley, N. R., Wszolek, Z. K., & Uitti, R. J. (2005). Gender and the Parkinson's disease phenotype. *Journal of Neurology*, 252, 1201–1205. <https://doi.org/10.1007/s00415-005-0835-7>
- Baldereschi, M., Di Carlo, A., Rocca, W. A., Vanni, P., Maggi, S., Perissinotto, E., Grigoletto, F., Amaducci, L., & Inzitari, D. (2000). Parkinson's disease and parkinsonism in a longitudinal study: Two-fold higher incidence in men. ILSA Working Group. *Italian Longitudinal Study on Aging. Neurology*, 55, 1358–1363. <https://doi.org/10.1212/WNL.55.9.1358>
- Bancroft, E. A., & Srinivasan, R. (2020). Quantifying spontaneous  $\text{Ca}^{2+}$  fluxes and their downstream effects in primary mouse midbrain neurons. *Journal of Visualized Experiments: Jove*, 163, e61481.
- Baraka, A. M., Korish, A. A., Soliman, G. A., & Kamal, H. (2011). The possible role of estrogen and selective estrogen receptor modulators in a rat model of Parkinson's disease. *Life Sciences*, 88, 879–885. <https://doi.org/10.1016/j.lfs.2011.03.010>
- Becker, J. B. (1990). Estrogen rapidly potentiates amphetamine-induced striatal dopamine release and rotational behavior during microdialysis. *Neuroscience Letters*, 118, 169–171. [https://doi.org/10.1016/0304-3940\(90\)90618-J](https://doi.org/10.1016/0304-3940(90)90618-J)
- Cai, P., Ye, J., Zhu, J., Liu, D., Chen, D., Wei, X., Johnson, N. R., Wang, Z., Zhang, H., Cao, G., Xiao, J., Ye, J., & Lin, L. I. (2016). Inhibition of endoplasmic reticulum stress is involved in the neuroprotective effect of bFGF in the 6-OHDA-induced Parkinson's disease model. *Aging and Disease*, 7, 336–449. <https://doi.org/10.14336/AD.2016.0117>
- Celardo, I., Costa, A. C., Lehmann, S., Jones, C., Wood, N., Mencacci, N. E., Mallucci, G. R., Loh, S. H., & Martins, L. M. (2016). Mitofusin-mediated ER stress triggers neurodegeneration in pink1/parkin models of Parkinson's disease. *Cell Death & Disease*, 7, e2271. <https://doi.org/10.1038/cddis.2016.173>
- Chao, O. Y., Huston, J. P., von Bothmer, A., & Pum, M. E. (2011). Chronic progesterone treatment of male rats with unilateral 6-hydroxydopamine lesion of the dorsal striatum exacerbates [corrected] parkinsonian symptoms. *Neuroscience*, 196, 228–236.
- Clemens, P., Baron, J. A., Coffey, D., & Reeves, A. (1995). The short-term effect of nicotine chewing gum in patients with Parkinson's disease. *Psychopharmacology (Berl)*, 117, 253–256. <https://doi.org/10.1007/BF02245195>
- Coe, J. W., Brooks, P. R., Vetelino, M. G. et al (2005). Varenicline: An alpha4beta2 nicotinic receptor partial agonist for smoking cessation. *Journal of Medicinal Chemistry*, 48, 3474–3477.
- Colla, E. (2019). Linking the endoplasmic reticulum to Parkinson's disease and alpha-synucleinopathy. *Frontiers in Neuroscience*, 13, 560. <https://doi.org/10.3389/fnins.2019.00560>
- Colla, E., Coune, P., Liu, Y., Pletnikova, O., Troncoso, J. C., Iwatsubo, T., Schneider, B. L., & Lee, M. K. (2012). Endoplasmic reticulum stress is important for the manifestations of alpha-synucleinopathy in vivo. *Journal of Neuroscience*, 32, 3306–3320.
- Colla, E., Jensen, P. H., Pletnikova, O., Troncoso, J. C., Glabe, C., & Lee, M. K. (2012). Accumulation of toxic alpha-synuclein oligomer within endoplasmic reticulum occurs in alpha-synucleinopathy in vivo. *Journal of Neuroscience*, 32, 3301–3305.
- Coppola-Segovia, V., Cavarsan, C., Maia, F. G., Ferraz, A. C., Nakao, L. S., Lima, M. M., & Zanata, S. M. (2017). ER stress induced by tunicamycin triggers alpha-synuclein oligomerization, dopaminergic neurons death and locomotor impairment: A new model of Parkinson's disease. *Molecular Neurobiology*, 54, 5798–5806.
- Dias, V., Junn, E., & Mouradian, M. M. (2013). The role of oxidative stress in Parkinson's disease. *Journal of Parkinson's Disease*, 3, 461–491. <https://doi.org/10.3233/JPD-130230>
- Dwivedi, A. K., Mallawaarachchi, I., & Alvarado, L. A. (2017). Analysis of small sample size studies using nonparametric bootstrap test with pooled resampling method. *Statistics in Medicine*, 36, 2187–2205. <https://doi.org/10.1002/sim.7263>
- Fernandes, H. J., Hartfield, E. M., Christian, H. C. et al (2016). ER stress and autophagic perturbations lead to elevated extracellular alpha-synuclein in GBA-N370S Parkinson's iPSC-derived dopamine neurons. *Stem Cell Reports*, 6, 342–356.
- Galindo, I., Hernaez, B., Munoz-Moreno, R., Cuesta-Geijo, M. A., Dalmau-Mena, I., & Alonso, C. (2012). The ATF6 branch of unfolded protein response and apoptosis are activated to promote African swine fever virus infection. *Cell Death & Disease*, 3, e341. <https://doi.org/10.1038/cddis.2012.81>
- Grealish, S., Mattsson, B., Draxler, P., & Bjorklund, A. (2010). Characterisation of behavioural and neurodegenerative changes induced by intranigral 6-hydroxydopamine lesions in a mouse model of Parkinson's disease. *European Journal of Neuroscience*, 31, 2266–2278. <https://doi.org/10.1111/j.1460-9568.2010.07265.x>
- Gully, J. C., Sergeyev, V. G., Bhootada, Y., Mendez-Gomez, H., Meyers, C. A., Zolotukhin, S., Gorbatyuk, M. S., & Gorbatyuk, O. S. (2016). Up-regulation of activating transcription factor 4 induces severe loss of dopamine nigral neurons in a rat model of Parkinson's disease. *Neuroscience Letters*, 627, 36–41. <https://doi.org/10.1016/j.neulet.2016.05.039>
- Hariz, G. M., Lindberg, M., Hariz, M. I., & Bergenheim, A. T. (2003). Gender differences in disability and health-related quality of life in patients with Parkinson's disease treated with stereotactic surgery. *Acta Neurologica Scandinavica*, 108, 28–37. <https://doi.org/10.1034/j.1600-0404.2003.00092.x>
- Heman-Ackah, S. M., Manzano, R., Hoozemans, J. J. M., Scheper, W., Flynn, R., Haerty, W., Cowley, S. A., Bassett, A. R., & Wood, M. J. A. (2017). Alpha-synuclein induces the unfolded protein response in Parkinson's disease SNCA triplication iPSC-derived neurons. *Human Molecular Genetics*, 26, 4441–4450. <https://doi.org/10.1093/hmg/ddx331>
- Henderson, B. J., Srinivasan, R., Nichols, W. A., Dilworth, C. N., Gutierrez, D. F., Mackey, E. D. W., McKinney, S., Drenan, R. M., Richards, C. I., & Lester, H. A. (2014). Nicotine exploits a COPI-mediated process for chaperone-mediated up-regulation of its receptors. *Journal of General Physiology*, 143, 51–66. <https://doi.org/10.1085/jgp.201311102>
- Henley, B. M., Cohen, B. N., Kim, C. H., Gold, H. D., Srinivasan, R., McKinney, S., Deshpande, P., & Lester, H. A. (2017). Reliable identification of living dopaminergic neurons in midbrain cultures using RNA sequencing and TH-promoter-driven eGFP expression. *Journal of Visualized Experiments: Jove*, 120, e54981. <https://doi.org/10.3791/54981>
- Hetz, C., & Papa, F. R. (2018). The unfolded protein response and cell fate control. *Molecular Cell*, 69, 169–181. <https://doi.org/10.1016/j.molcel.2017.06.017>

- Hetz, C., & Saxena, S. (2017). ER stress and the unfolded protein response in neurodegeneration. *Nature Reviews. Neurology*, 13, 477–491. <https://doi.org/10.1038/nrneurol.2017.99>
- Holtz, W. A., & O'Malley, K. L. (2003). Parkinsonian mimetics induce aspects of unfolded protein response in death of dopaminergic neurons. *Journal of Biological Chemistry*, 278, 19367–19377. <https://doi.org/10.1074/jbc.M211821200>
- Hoozemans, J. J., van Haastert, E. S., Eikelenboom, P., de Vos, R. A., Rozemuller, J. M., & Scheper, W. (2007). Activation of the unfolded protein response in Parkinson's disease. *Biochemical and Biophysical Research Communications*, 354, 707–711. <https://doi.org/10.1016/j.bbrc.2007.01.043>
- Hoozemans, J. J., van Haastert, E. S., Nijholt, D. A., Rozemuller, A. J., & Scheper, W. (2012). Activation of the unfolded protein response is an early event in Alzheimer's and Parkinson's disease. *Neuro-Degenerative Diseases*, 10, 212–215. <https://doi.org/10.1159/000334536>
- Hu, L. W., Yen, J. H., Shen, Y. T., Wu, K. Y., & Wu, M. J. (2014). Luteolin modulates 6-hydroxydopamine-induced transcriptional changes of stress response pathways in PC12 cells. *PLoS One*, 9, e97880. <https://doi.org/10.1371/journal.pone.0097880>
- Lammers, C. H., D'Souza, U., Qin, Z. H., Lee, S. H., Yajima, S., & Mouradian, M. M. (1999). Regulation of striatal dopamine receptors by estrogen. *Synapse (New York, N. Y.)*, 34, 222–227. [https://doi.org/10.1002/\(SICI\)1098-2396\(19991201\)34:3<222::AID-SYN6>3.0.CO;2-J](https://doi.org/10.1002/(SICI)1098-2396(19991201)34:3<222::AID-SYN6>3.0.CO;2-J)
- Lee, J., Pinares-Garcia, P., Loke, H., Ham, S., Vilain, E., & Harley, V. R. (2019). Sex-specific neuroprotection by inhibition of the Y-chromosome gene, SRY, in experimental Parkinson's disease. *Proceedings of the National Academy of Sciences of the United States of America*, 116, 16577–16582.
- Lemay, S., Blanchet, P., Chouinard, S., Masson, H., Soland, V., & Bedard, M. A. (2003). Poor tolerability of a transdermal nicotine treatment in Parkinson's disease. *Clinical Neuropharmacology*, 26, 227–229. <https://doi.org/10.1097/00002826-200309000-00004>
- Ma, C., Liu, Y., Neumann, S., & Gao, X. (2017). Nicotine from cigarette smoking and diet and Parkinson disease: A review. *Translational Neurodegeneration*, 6, 18. <https://doi.org/10.1186/s40035-017-0090-8>
- Maris, E. (2012). Statistical testing in electrophysiological studies. *Psychophysiology*, 49, 549–565. <https://doi.org/10.1111/j.1469-8986.2011.01320.x>
- McFarland, K., Price, D. L., Davis, C. N., Ma, J. N., Bonhaus, D. W., Burstein, E. S., & Olsson, R. (2013). AC-186, a selective nonsteroidal estrogen receptor beta agonist, shows gender specific neuroprotection in a Parkinson's disease rat model. *ACS Chemical Neuroscience*, 4, 1249–1255.
- Mercado, G., Castillo, V., Soto, P., & Sidhu, A. (2016). ER stress and Parkinson's disease: Pathological inputs that converge into the secretory pathway. *Brain Research*, 1648, 626–632. <https://doi.org/10.1016/j.brainres.2016.04.042>
- Mercado, G., Valdes, P., & Hetz, C. (2013). An ERcentric view of Parkinson's disease. *Trends in Molecular Medicine*, 19, 165–175. <https://doi.org/10.1016/j.molmed.2012.12.005>
- Nakanishi, K., Sudo, T., & Morishima, N. (2005). Endoplasmic reticulum stress signaling transmitted by ATF6 mediates apoptosis during muscle development. *Journal of Cell Biology*, 169, 555–560. <https://doi.org/10.1083/jcb.200412024>
- Quick, Q. A., & Faison, M. O. (2012). CHOP and caspase 3 induction underlie glioblastoma cell death in response to endoplasmic reticulum stress. *Experimental and Therapeutic Medicine*, 3, 487–492. <https://doi.org/10.3892/etm.2011.422>
- Richards, C. I., Luong, K., Srinivasan, R., Turner, S. W., Dougherty, D. A., Korlach, J., & Lester, H. A. (2012). Live-cell imaging of single receptor composition using zero-mode waveguide nanostructures. *Nano Letters*, 12, 3690–3694. <https://doi.org/10.1021/nl301480h>
- Richards, C. I., Srinivasan, R., Xiao, C., Mackey, E. D., Miwa, J. M., & Lester, H. A. (2011). Trafficking of alpha4\* nicotinic receptors revealed by supercliptic phluorin: Effects of a beta4 amyotrophic lateral sclerosis-associated mutation and chronic exposure to nicotine. *Journal of Biological Chemistry*, 286, 31241–31249.
- Ryu, E. J., Harding, H. P., Angelastro, J. M., Vitolo, O. V., Ron, D., & Greene, L. A. (2002). Endoplasmic reticulum stress and the unfolded protein response in cellular models of Parkinson's disease. *The Journal of Neuroscience*, 22, 10690–10698. <https://doi.org/10.1523/JNEUROSCI.22-24-10690.2002>
- Silva, R. M., Ries, V., Oo, T. F., Yarygina, O., Jackson-Lewis, V., Ryu, E. J., Lu, P. D., Marciniak, S. J., Ron, D., Przedborski, S., Kholodilov, N., Greene, L. A., & Burke, R. E. (2005). CHOP/GADD153 is a mediator of apoptotic death in substantia nigra dopamine neurons in an in vivo neurotoxin model of parkinsonism. *Journal of Neurochemistry*, 95, 974–986. <https://doi.org/10.1111/j.1471-4159.2005.03428.x>
- Srinivasan, R., Henley, B. M., Henderson, B. J., Indersmitten, T., Cohen, B. N., Kim, C. H., McKinney, S., Deshpande, P., Xiao, C., & Lester, H. A. (2016). Smoking-relevant nicotine concentration attenuates the unfolded protein response in dopaminergic neurons. *Journal of Neuroscience*, 36, 65–79. <https://doi.org/10.1523/JNEUROSCI.2126-15.2016>
- Srinivasan, R., Huang, B. S., Venugopal, S., Johnston, A. D., Chai, H., Zeng, H., Golshani, P., & Khakh, B. S. (2015). Ca(2+) signaling in astrocytes from Ip3r2(-/-) mice in brain slices and during startle responses in vivo. *Nature Neuroscience*, 18, 708–717. <https://doi.org/10.1038/nn.4001>
- Srinivasan, R., Lu, T. Y., Chai, H., Xu, J., Huang, B. S., Golshani, P., Coppola, G., & Khakh, B. S. (2016). New transgenic mouse lines for selectively targeting astrocytes and studying calcium signals in astrocyte processes in situ and in vivo. *Neuron*, 92, 1181–1195.
- Srinivasan, R., Pantoja, R., Moss, F. J., Mackey, E. D., Son, C. D., Miwa, J., & Lester, H. A. (2011). Nicotine up-regulates alpha4beta2 nicotinic receptors and ER exit sites via stoichiometry-dependent chaperoning. *Journal of General Physiology*, 137, 59–79.
- Srinivasan, R., Richards, C. I., Xiao, C., Rhee, D., Pantoja, R., Dougherty, D. A., Miwa, J. M., & Lester, H. A. (2012). Pharmacological chaperoning of nicotinic acetylcholine receptors reduces the endoplasmic reticulum stress response. *Molecular Pharmacology*, 81, 759–769. <https://doi.org/10.1124/mol.112.077792>
- Subramanian, A., Capalbo, A., Iyengar, N. R., Rizzo, R., di Campli, A., Di Martino, R., Lo Monte, M., Beccari, A. R., Yerudkar, A., del Vecchio, C., Glielmo, L., Turacchio, G., Pirozzi, M., Kim, S. G., Henklein, P., Cancino, J., Parashuraman, S., Diviani, D., Fanelli, F., ... Luini, A. (2019). Auto-regulation of secretory flux by sensing and responding to the folded cargo protein load in the endoplasmic reticulum. *Cell*, 176(6), 1461–1476.e23. <https://doi.org/10.1016/j.cell.2019.01.035>
- Surmeier, D. J. (2018). Determinants of dopaminergic neuron loss in Parkinson's disease. *The FEBS Journal*, 285, 3657–3668. <https://doi.org/10.1111/febs.14607>
- Teske, B. F., Fusakio, M. E., Zhou, D., Shan, J., McClintick, J. N., Kilberg, M. S., & Wek, R. C. (2013). CHOP induces activating transcription factor 5 (ATF5) to trigger apoptosis in response to perturbations in protein homeostasis. *Molecular Biology of the Cell*, 24, 2477–2490. <https://doi.org/10.1091/mbc.e13-01-0067>
- Tozzi, A., de Lure, A., Tantucci, M., Durante, V., Quiroga-Varela, A., Giampà, C., Di Mauro, M., Mazzocchetti, P., Costa, C., Di Filippo, M., & Grassi, S. (2015). Endogenous 17beta-estradiol is required for activity-dependent long-term potentiation in the striatum: Interaction with the dopaminergic system. *Frontiers in Cellular Neuroscience*, 9, 192.
- Tutka, P., Vinnikov, D., Courtney, R. J., & Benowitz, N. L. (2019). Cytisine for nicotine addiction treatment: A review of pharmacology, therapeutics and an update of clinical trial evidence for smoking cessation. *Addiction*, 114, 1951–1969. <https://doi.org/10.1111/add.14721>
- Tutka, P., & Zatonski, W. (2006). Cytisine for the treatment of nicotine addiction: From a molecule to therapeutic efficacy. *Pharmacological Reports*, 58, 777–798.





- Ueno, M., Kakinuma, Y., Yuhki, K., Murakoshi, N., Iemitsu, M., Miyauchi, T., & Yamaguchi, I. (2006). Doxorubicin induces apoptosis by activation of caspase-3 in cultured cardiomyocytes in vitro and rat cardiac ventricles in vivo. *Journal of Pharmacological Sciences*, 101, 151–158. <https://doi.org/10.1254/jphs.FP0050980>
- Viergege, A., Sieberer, M., Jacobs, H., Hagenah, J. M., & Viergege, P. (2001). Transdermal nicotine in PD: A randomized, double-blind, placebo-controlled study. *Neurology*, 57, 1032–1035. <https://doi.org/10.1212/WNL.57.6.1032>
- Villafane, G., Cesaro, P., Rialland, A., Baloul, S., Azimi, S., Bourdet, C., Le Houezec, J., Macquin-Mavier, I., & Maison, P. (2007). Chronic high dose transdermal nicotine in Parkinson's disease: An open trial. *European Journal of Neurology*, 14, 1313–1316. <https://doi.org/10.1111/j.1468-1331.2007.01949.x>
- Villafane, G., Thiriez, C., Audureau, E., Straczek, C., Kerschen, P., Cormier-Dequaire, F., Van Der Gucht, A., Gurruchaga, J.-M., Quéré-Carne, M., Evangelista, E., Paul, M., Defer, G., Damier, P., Remy, P., Itti, E., & Fénelon, G. (2018). High-dose transdermal nicotine in Parkinson's disease patients: A randomized, open-label, blinded-endpoint evaluation phase 2 study. *European Journal of Neurology*, 25, 120–127. <https://doi.org/10.1111/ene.13474>
- Walter, P., & Ron, D. (2011). The unfolded protein response: From stress pathway to homeostatic regulation. *Science*, 334, 1081–1086. <https://doi.org/10.1126/science.1209038>
- Wang, H., Dong, Y., Zhang, J., Xu, Z., Wang, G., Swain, C. A., Zhang, Y., & Xie, Z. (2014). Isoflurane induces endoplasmic reticulum stress and caspase activation through ryanodine receptors. *British Journal of Anaesthesia*, 113, 695–707. <https://doi.org/10.1093/bja/aeu053>
- Wang, H. Q., & Takahashi, R. (2007). Expanding insights on the involvement of endoplasmic reticulum stress in Parkinson's disease. *Antioxidants & Redox Signaling*, 9, 553–561. <https://doi.org/10.1089/ars.2006.1524>
- Wedenberg, M. (2013). Assessing the uncertainty in QUANTEC's dose-response relation of lung and spinal cord with a bootstrap analysis. *International Journal of Radiation Oncology Biology Physics*, 87, 795–801. <https://doi.org/10.1016/j.ijrobp.2013.06.2040>
- Wei, L., Surma, M., Gough, G., Shi, S., Lambert-Cheatham, N., Chang, J., & Shi, J. (2015). Dissecting the mechanisms of doxorubicin and oxidative stress-induced cytotoxicity: The involvement of actin cytoskeleton and ROCK1. *PLoS One*, 10, e0131763. <https://doi.org/10.1371/journal.pone.0131763>
- Xie, L., Tiong, C. X., & Bian, J. S. (2012). Hydrogen sulfide protects SH-SY5Y cells against 6-hydroxydopamine-induced endoplasmic reticulum stress. *American Journal of Physiology-Cell Physiology*, 303, C81–91. <https://doi.org/10.1152/ajpcell.00281.2011>
- Xiong, Y., Chen, H., Lin, P., Wang, A., Wang, L., & Jin, Y. (2017). ATF6 knockdown decreases apoptosis, arrests the S phase of the cell cycle, and increases steroid hormone production in mouse granulosa cells. *American Journal of Physiology-Cell Physiology*, 312, C341–C353. <https://doi.org/10.1152/ajpcell.00222.2016>
- Yunes, R., Casas, S., Gaglio, E., & Cabrera, R. (2015). Progesterone exerts a neuromodulatory effect on turning behavior of hemiparkinsonian male rats: Expression of 3 alpha -hydroxysteroid oxidoreductase and allopregnanolone as suggestive of gabaa receptors involvement. *Parkinson's Disease*, 2015, 431690.
- Zeng, L., Zampetaki, A., Margariti, A., Pepe, A. E., Alam, S., Martin, D., Xiao, Q., Wang, W., Jin, Z.-G., Cockerill, G., Mori, K., Li, Y.-s J., Hu, Y., Chien, S., & Xu, Q. (2009). Sustained activation of XBP1 splicing leads to endothelial apoptosis and atherosclerosis development in response to disturbed flow. *Proceedings of the National Academy of Sciences of the United States of America*, 106, 8326–8331. <https://doi.org/10.1073/pnas.0903197106>
- Zhou, Z., Ribas, V., Rajbhandari, P. et al (2018). Estrogen receptor alpha protects pancreatic beta-cells from apoptosis by preserving mitochondrial function and suppressing endoplasmic reticulum stress. *Journal of Biological Chemistry*, 293, 4735–4751.

## SUPPORTING INFORMATION

Additional supporting information may be found online in the Supporting Information section.

**How to cite this article:** Zarate SM, Pandey G, Chilukuri S, et al. Cytisine is neuroprotective in female but not male 6-hydroxydopamine lesioned parkinsonian mice and acts in combination with 17- $\beta$ -estradiol to inhibit apoptotic endoplasmic reticulum stress in dopaminergic neurons. *J Neurochem*. 2021;157:710–726. <https://doi.org/10.1111/jnc.15282>